Journal of Molecular Structure 1248 (2022) 131347

Contents lists available at ScienceDirect

Journal of Molecular Structure

journal homepage: www.elsevier.com/locate/molstr

Isomerism, molecular structure, and vibrational assignment of tris(triflouroacetylacetonato)iron(III): An experimental and theoretical study

Farzad Gandomi, Mohammad Vakili*, Reza Takjoo, Sayyed Faramarz Tayyari

Department of Chemistry, Faculty of Science, Ferdowsi University of Mashhad, Mashhad, Iran

ARTICLE INFO

Article history:
Received 23 May 2021
Revised 2 August 2021
Accepted 19 August 2021
Available online 23 August 2021

Keywords:
Vibrational spectroscopy
DFT
UV spectra
Tris(triflouroacetylacetonato)iron(III)
Tris(acetylacetonate) iron(III)

ABSTRACT

The isomerism, optimized molecular structure, UV spectrum, metal-ligand bond strength, and vibrational assignment of tris(triflouroacetylacetonato)iron(III), $Fe(TFAA)_3$, were investigated by the aid of theoretical calculations (using DFT and Atoms-in-Molecules (AIM) at the B3LYP/6-311++G(d,p) level) and experimental methods (vibrational and UV spectroscopy). To explore the effect of the CF_3 substituent in the β-position on the properties of complex, the above theoretical and experimental results of the titled complex compared with the corresponding data for tris(acetylacetonato) iron(III), $Fe(AA)_3$. Both theoretical and experimental results confirmed that there is no significant difference in the strength of the Fe−O bond in these complexes. The effect of the CF_3 group on the experimental vibrational bands of the chelated ring agrees with the calculated results. Comparing the observed and calculated vibrational spectra suggests that vibrational spectroscopy cannot be used to determine the type of isomer in the sample. However, due to the small difference of energy between the fac and mer isomers in the $Fe(TFAA)_3$, the presence of both isomers in the sample is possible. The computed quantum chemical descriptors of $Fe(TFAA)_3$ and $Fe(AA)_3$ were also compared.

1. Introduction

The β-diketones (1,3-diketones) bear two carbonyl groups separated by one carbon atom (α-carbon) [1]. The substituents on the carbonyl functional can be an alkyl, a fluorinated alkyl, an aromatic, or a heteroaromatic group [2–4]. The simplest β-diketone is acetylacetone (AA), where the substituents on both carbonyl groups are methyl groups. All other β-diketones can be considered as derived from acetylacetone by substitution of the CH_3 groups by other groups. The enolic hydrogen atom can be replaced by metal cation under appropriate conditions. Triflouroacetylacetone (TFAA), one of the ligands studied in this work, was used in the extraction of several metals such as Cu, Ni, Co, and Fe [5,6].

The experimental structures for some trivalent metals with acetylacetone and triflouroacetylacetone ligands were recognized [7–12]. Kato and Gohda have investigated the magnetic circular dichroism (MCD) of $M(AA)_3$and $M(AA)_2$, that M = Cu, Fe, and Co [13]. Conradie et al. characterized complexes of iron with 2,4-pentanedione (AA), 1-phenyl-1,3-butanedione (BA), 4,4,4-trifluoro-1-(2-thienyl)-1,3-butanedione (HTTA), and 4,4,4-Trifluoro-1-(2-furyl)-1,3-butanedione (TTFU) by DFT, elemental analyses, FT-IR, and UV-Vis techniques [14,15]. Conradie and Tachikawa et al. studied iron (III) complexes with the mentioned ligands by DFT calculations and experimental cyclic voltammetry measurements [16,17]. Metal acetylacetonates, as nontoxic precursors, were used for the synthesis of transition metal oxide nanoparticles [18].

The structure, isomerism, vibrational spectra, and metal-ligand strength of numerous metal β-diketonate complexes have been studied [19–32]. Despite general studies, there are a few reported works about the vibrational analysis of β-substituted trivalent complexes [3–7,14–16,33–38]. The DFT methods showed an agreement with the experiment results, tris(β-diketonato)iron(III) complexes are stable molecules with the metal in a high spin state ($d_{z2}{}^1 d_{xy}{}^1 d_{yz}{}^1 d_{xz}{}^1 d_{x2-y2}{}^1$, $S = 5/2$) [14,34–36,39].

Diaz-Acosta et al. [40,41] reported the IR spectra for $Fe(AA)_3$ and its deuterated analogous. Jayasooriya et al. [42] reported the vibrational spectra of $Fe(AA)_3$, using IR, Raman, and nuclear inelastic spectroscopy. The crystal structure of ferric acetylacetonate has been determined [10,43,44]. The structure, isomerism, vibrational assignment, and metal-ligand strength of the title molecule, tris(triflouroacetylacetonato)iron(III), $Fe(TFAA)_3$, were not reported previously. Therefore, the study of this molecule and comparing it with $Fe(AA)_3$, could be valuable materials from the scientific point of view.

* Corresponding author.
E-mail address: Vakili-m@um.ac.ir (M. Vakili).

https://doi.org/10.1016/j.molstruc.2021.131347
0022-2860/

This work aims to compare the structure and vibrational assignment of $Fe(TFAA)_3$ with those for $Fe(AA)_3$. This comparison is performed with the aid of DFT calculations and IR, Raman, and UV-Vis spectroscopy. By comparing the Fe−O bond strength of $Fe(TFAA)_3$ and $Fe(AA)_3$ it is possible to explore the effect of the CF_3 substitution on the metal-O bond strength of the complex. For better accuracy of vibrational assignments, the vibrational spectra of both complexes are compared with those of aluminum trifluoroacetylacetonate, $Al(TFAA)_3$, and $Cr(AA)_3$ [3,33].

2. Methodology

2.1. Method of analysis

All the calculations are performed using Gaussian 09W software [45]. The geometry optimization, vibrational frequencies of $Fe(TFAA)_3$ and $Fe(AA)_3$ obtained at the B3LYP [46–48] level, using 6-311++G(d,p) basis set. Raman activities of the mentioned complexes were computed at the same level of calculation, using standard procedures (Freq = Raman). Vibrational assignments have been achieved based on the comparison of calculated and observed Raman and IR spectra and their intensities. The assignments of observed wavenumbers are aided by the animation of GaussView 6.0 visualization [49]. The zero-point vibrational energy, ZPE, was obtained by using the results of frequency calculations. The topological parameters such as the electron density and Laplacian of electron density at the critical points of Fe−O bonds are evaluated using the AIM 2000 [50] software. The HOMO and LUMO were obtained at the same level of calculations.

The Potential Energy Distribution (PED) of all normal modes calculated by VEDA 4.0 program via optimization method [51]. According to reported work by Jamróz and Darugar et al., the optimization method improved the PED contributions [52,53].

2.2. Experimental

Synthesis of the iron (III) β-diketone complexes with trifluoroacetylacetone and acetylacetone ligands.

1,1,1-trifluoro-2,4-pentanedione and 2,4-pentanedioneas ligands and the other compounds including iron (III) chloride hexahydrate, sodium acetate, and ammonia for synthesis were purchased from Alfa Aesar and Merck companies. The $Fe(TFAA)_3$ and $Fe(AA)_3$ complexes are prepared according to the similar procedures described by Fay and Chaudhuri et al. [54,55]. For this purpose, an aqueous solution (10 ml) containing iron (III) chloride hexahydrate (10 mmol, 2.70 g) and sodium acetate (0.5 g) was shaken with 1,1,1-trifluoro-2,4-pentanedione (30 mmol, 3.60 ml) in 20 ml of ethanol. After passing about 30 min, red crystalline solids which had precipitated, washed with distillated water then were filtered and dried under vacuum. The $Fe(AA)_3$ complex was synthesized according to the mentioned method too. The melting points of the light and dark red solids of $Fe(AA)_3$ and $Fe(TFAA)_3$ are 178 and 108 °C, respectively. These melting points are near to those reported in the literature, 179 °C for $Fe(TFAA)_3$ and 111 °C for $Fe(AA)_3$ [56,57]. Calculated m/z = 515.09 for $C_{15}H_{12}F_9FeO_6$ $[Fe(TFAA)_3]^+$; founded: m/z = 514.0, see Fig. S1, Supplementary materials.

2.3. Instruments analyses

The infrared spectra in the 4000–500 cm^{-1} region were recorded on a Bomem MB-154 Fourier transform spectrophotometer using KBr pellets and CCl_4 solution. The spectra were collected with a resolution of 4 cm^{-1} by signal averaging the results of 15 scans.

The Far-IR spectra in the region 700–250 cm^{-1} were obtained using a Thermo Nicolet NEXUS 870 FT-IR spectrometer equipped with a DTGS/polyethylene detector and a solid substrate beam splitter with the use of polyethylene disks. The spectra were collected with a resolution of 4 cm^{-1} by signal averaging the results of 32 scans.

For $Fe(TFAA)_3$, Raman measurements were performed by Horiba XploRA Raman spectrometer equipped with a confocal microscope. The laser excitation of 785 nm with grating 1800 grooves/mm was employed in a spectral range of 1700–300 cm^{-1}.

The UV spectra were examined in the range of 200–400 nm at 298 K using a Perkin Elmer Lambda 25 spectrophotometer. The complexes were dissolved in C_2H_5OH as the solvent.

The mass analysis was achieved on a Varian Mat CH-7 at 70 eV.

3. Results and discussion

3.1. Structure and isomerism

In the reported works, the most stable electronic spin for $Fe(AA)_3$ is considered as 5/2, so its multiplicity is 6 [14,41]. According to the results of the calculations at the B3LYP/6-311++G(d,p) level, we also confirmed the value of 6 for multiplicity as the most stable multiplicity for the understudy complexes, see Table S1 (supplementary material). In $Fe(TFAA)_3$ the relative energies for other multiplicities, 2 and 4, are 9.9–14.7 kcal/mol more than that of multiplicity 6. According to the calculation results, the symmetry of $Fe(AA)_3$ and $Fe(TFAA)_3$ complexes is D_3 and C_1 (C_3), respectively, with sextet multiplicity. This symmetry and multiplicity agree with the reported work by Diaz-Acosta et al. studies for $Fe(AA)_3$ [41]. The C_1 and C_3 point groups are due to mer and fac isomers, respectively.

The optimized structure of $Fe(AA)_3$ and $Fe(TFAA)_3$ and their numbering are shown in Fig. 1. Theoretically, two isomers suggested for $Fe(TFAA)_3$ complex, as fac and mer isomers, see Fig. 1. The calculation results in the gas phase show that the relative energy of fac isomer of $Fe(TFAA)_3$ is 0.54 kcal/mol more than the mer isomer, and ZPE correction does not affect this energy difference. Therefore, the coexistence of both isomers can be considered in the gas phase. The calculated energy difference was obtained for the multiplicity of 6.

The optimized parameters along with their experimental structure of $Fe(AA)_3$ [10,41,58] and the calculation results of $Fe(TFAA)_3$ isomers, along with their averaged values, are compared in Table 1. According to this table, the calculated structure of $Fe(AA)_3$ is similar to that by Diaz-Acosta et al. [41]. Also, the gas-phase electron diffraction (GED) results [58] are in agreement with the calculated structure.

As Table 1 shows, the averaged Fe−O bond length in both fac and mer isomers of $Fe(TFAA)_3$ is slightly shorter than those in $Fe(AA)_3$. This small difference in Fe−O bond strength is also confirmed with the other bond lengths of the chelated ring and AIM calculation results too, see Table 1. So, the comparison of these averaged values with the calculated Fe−O bond length indicates that there is no significant difference in Fe−O bond strength. This result is also confirmed by the experimental UV results.

Also, Table 1 shows that the $C-C_{Met}$ bond lengths of $Fe(TFAA)_3$ are higher than those in $Fe(AA)_3$, which is consistent with Zahedi-Tabrizi and Tayyari et al. works [59,60]. In addition, due to the electron-withdrawing effect of the CF_3 group, the $C-CF_3$ bond length of $Fe(TFAA)_3$ is longer than that of $Fe(AA)_3$. This elongation could be explained by the electron-withdrawing effect of the CF_3 group. In this view, the attractive interaction in $C^{\delta+}-C^{\delta-}$ of $C-CH_3$ becomes repulsive ($C^{\delta+}-C^{\delta}+$), if the hydrogen atoms of the methyl group replaced by the fluorine atoms. On the other hand, the $C_{\alpha}-CCF_3$ bond length in $Fe(TFAA)_3$ is shorter than the corresponding value in $Fe(AA)_3$. This shortening is also caused by the same effect the carbon atom attached to the CF_3 group is more

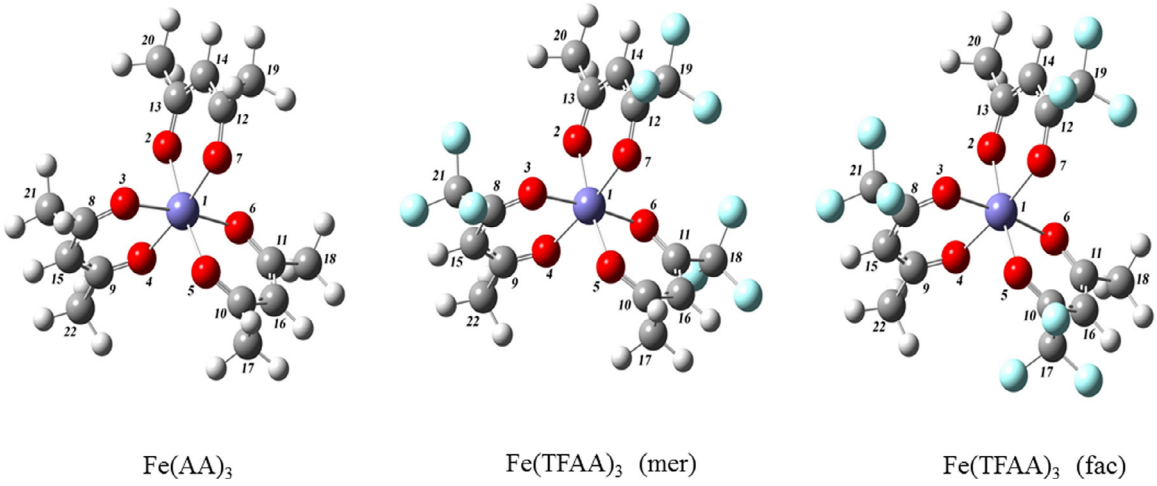

Fig. 1. The optimized structure of $Fe(AA)_3$ and $Fe(TFAA)_3$, mer and fac, complexes and their numbering of the atoms.

Table 1
Some selected theoretical and experimental geometrical parameters of $Fe(AA)_3$ and $Fe(TFAA)_3$ (fac and mer) calculated at B3LYP/6-311++G(d,p) level of theory (bond lengths and bond angles are in Å and °, respectively.

Parameters	$Fe(TFAA)_3$				$Fe(AA)_3$				
	Theoretical				Theoretical		Exp.♣ [58]	Exp. [41]	Exp. [10]
Configuration	mer		fac		(This	Ref.			
Symmetry	(C_1)	Avg.	(C_3)	Avg.	work)	[41]	(D_3)		(C_1)
Bond angles									
Fe−O2	2.021	2.024	2.025	2.024	2.026	2.011	2.018	1.992	2.004
Fe−O7	2.027		2.023						1.993
Fe−O5	2.019	2.024	2.025	2.024					1.983
Fe−O6	2.029		2.023						1.976
Fe−O3	2.027	2.025	2.025	2.024					1.998
Fe−O4	2.022		2.023						2.000
O=CCF_3	1.265	1.266	1.265	1.266					
O=CCH_3	1.267		1.267		1.271	1.275	1.268	1.262	1.262*
C−CCF_3	1.387	1.401	1.388	1.401					
C−C_{Met}	1.414		1.414		1.404	1.405	1.399	1.382	1.382*
C−CF_3	1.543	1.525	1.543	1.525					
C−CH_3	1.506		1.506		1.511	1.512	1.507	1.504	1.504*
O2…O7	2.743	2.74	2.743	2.743	2.749		—	—	2.753*
O5…O6	2.741		2.743			—-	-	-	
O3…O4	2.737		2.743						
C−Hα	1.079		1.079		1.081	—-	1.070	—-	0.947*
R^2	—		—-		—-	—-	0.9999	—-	0.9949
Bond angles									
O2FeO7	85.2	85.2	85.3	85.3	85.4	87.1	87.4	87.4	87.8
O5FeO6	85.3		85.3						86.6
O3FeO4	85.1		85.3						87.9
O6/O5C$\beta$$CF_3$	113		113						
O5/O6C$\beta$$CH_3$	116.3		116.3		115.6	—-	115.9	—-	115.3*
O3Cβ8Cα15	127.8		127.7						
O4Cβ9Cα15	123.7		123.8		124.6	124.9	—-	124.5	124.5*
FeO7Cβ12	129		129.1						
FeO4Cβ9	132.2		132.1		131.0	129.8	129.0	129.1	129.1*
Cβ12Cα14Cβ13	121.9	121.8	121.8	121.8	123.4	123.5	123.2	124.8	124.8*
Cβ10Cα16Cβ11	121.8		121.8						
Cβ8Cα15Cβ9	121.7		121.8						
AIM [a]									
ρ_{BCP}	0.0779		0.0774		0.0774	—-	—	—	—
∇^2	-0.0980		-0.0971		-0.0976	—-	-	-	-
R^2	—		—-		—-	—-	0.9990	—-	0.9937

[a] The units of AIM results are: the density of critical point, ρ, (e.au^{-3}), the Laplacian of critical point, $\nabla^2\rho$, (e.au^{-5}).
* Due to the complex asymmetry, these values are different in each ligand and their averages are presented in the table.
♣ Experimental results reported from GED analysis.

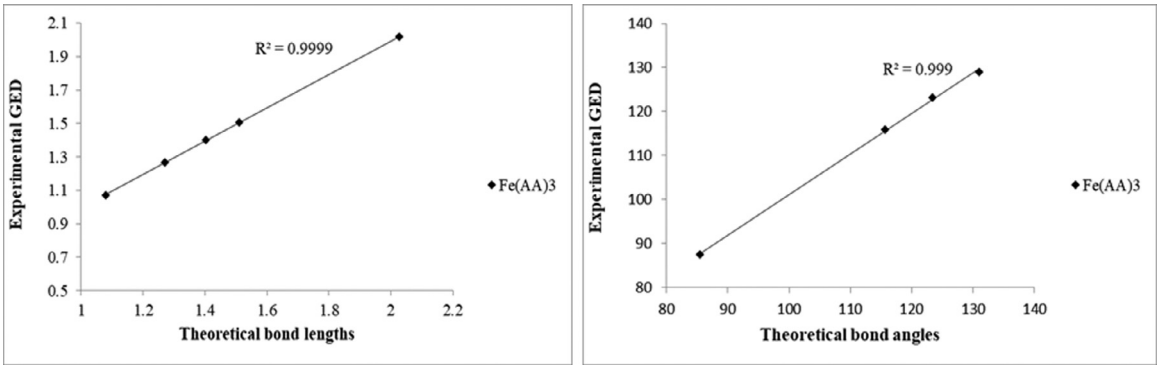

Fig. 2. The correlation between theoretical and reported experimental GED structure of $Fe(AA)_3$.

positive while the C_α atom is negative, which causes shortening of C_α−C bond length.

According to the AIM results in Table 1, the average of density (ρ) and its Laplacian ($\nabla^2\rho$) at metal-oxygen bond critical point in $Fe(TFAA)_3$ are 0.0776 and 0.0976, respectively. The mentioned values do not important change in comparison to $Fe(AA)_3$. These values indicate that the effect of CF_3 subgroup is negligible and has no significant effect on the metal-ligand bond strength, which is in agreement with other results including UV and vibrational analyzes.

The most stable form of $Fe(AA)_3$, with six multiplicity, has been used to compare with the experimental reported structure [13]. The regression coefficient parameter (R^2) between theoretical bond lengths and bond angles with the reported experimental, GED and X-ray, for $Fe(AA)_3$ are given in Figs. 2 and S2, supplementary materials. The regression coefficients of $Fe(AA)_3$ with GED are 0.9999 and 0.9990 for bond lengths and bond angles, respectively. Also, the mentioned R^2 values with X-ray were obtained as 0.9949 and 0.9937. The higher *R* square values of GED correlation respect to X-ray can be related to intermolecular interactions existent within crystal which are absent in the theoretical gas-phase geometry and experimental gas electron diffraction structure [61].

3.2. Experimental sections

3.2.1. UV spectra and frontier molecular orbital analyzes

In the present work, we have calculated the HOMO (the highest occupied molecular orbital) and LUMO (the lowest unoccupied molecular orbital) energies [62,63] for optimized structures of $Fe(AA)_3$ and both isomers of $Fe(TFAA)_3$. The 3D plots of frontier molecular orbital of the under studied metal complexes are shown in Fig. 3. The difference of HOMO-LUMO energy gap of $Fe(AA)_3$ is a little more than that of fac and mer. Accordingly, the HOMO→LUMO transition implies an electron density transfer for $Fe(AA)_3$ and fac of $Fe(TFAA)_3$ from π-conjugated of all three chelating rings to the metal-ligand regions of LUMO orbital, while transition for mer of $Fe(TFAA)_3$ is from two chelating rings of HOMO orbital to LUMO orbital, see Fig. 3.

The experimental UV spectra of both complexes are shown in Fig.4. The recorded UV spectrum of the $Fe(AA)_3$ complex shows a maximum absorption peak at 270 nm, but this band in $Fe(TFAA)_3$ is shown at 285 nm, which its red shift is in agreement with increasing of π conjugation transition and lowering band gap of this complex, in comparison to $Fe(AA)_3$. Additionally, the UV spectra of both complexes indicate the presence of a low-intensity band at 210 nm, which is due to Fe to oxygen charge transfer. The similarity of the wavelengths of this peak for both complexes is in agreement with the small difference of metal-ligand strength that is obtained by molecular structure. Also, the recording UV spectra are repeated in water solvent and the wavelengths do not show any significant difference in water respect to the ethanol. Hence it seems that the solvent has not effect on the transitions.

Table 2
Quantum chemical descriptor parameters for $Fe(AA)_3$ and $Fe(TFAA)_3$ isomers.

Property	$Fe(AA)_3$	mer-$Fe(TFAA)_3$	fac-$Fe(TFAA)_3$
E_{HOMO} (eV)	-6.33	-7.38	-7.40
E_{LUMO} (eV)	-1.32	-2.56	-2.56
Energy gap (eV)	5.01	4.82	4.84
Electronegativity (χ)	-2.5	-2.41	-2.42
Global hardness (η)	2.5	2.41	2.42
Chemical potential (μ)	3.83	4.97	4.98
Global electrophilicity (ω)	2.93	1.16	1.21
Chemical softness *S* (eV^{-1})	0.20	0.21	0.21
Dipole moment (Debye)	4.67	3.92	3.93

χ = - [E(LUMO)- E(HOMO)]/2; μ = [E(LUMO) + E(HOMO)]/2; η = [E(LUMO) - E(HOMO)]/2;$S = \frac{1}{2}\eta$; $\omega = \mu^2/2\eta$.

From the DFT calculations, different descriptors such as E_{HOMO}, E_{LUMO}, energy gap, global hardness (η), softness (*S*), electrophilicity index (ω), were considered to compare the structure-activity relationship (SAR) of the mentioned complexes [64,65]. The computed quantum chemical descriptors established upon DFT results are listed in Table 2. E_{HOMO} measures the electron-donating role of a complex, whilst E_{LUMO} measures its electron-accepting role. Therefore, the bigger the E_{HOMO} corresponds to the larger electron-donating ability, and the smaller the E_{LUMO} is related to the lower the resistance to accept electrons. The more softness indicates the more chemical activity. The electrophilicity index has lately been recognized as a factor of biological activity. According to Table 2, the electrophilicity (ω) of $Fe(AA)_3$ (2.93) is more than that of $Fe(TFAA)_3$ (about 1.20). So, the $Fe(AA)_3$ complex shows more electrophilicity attack strength. Besides, the chemical potentials (μ) of $Fe(TFAA)_3$ about 5.0 is larger than that 3.83 value for $Fe(AA)_3$. Hence, the reactivity property of $Fe(TFAA)_3$ is more than that $Fe(AA)_3$.

3.2.2. Vibrational analysis

The shortened and full assignment along to PEDs of $Fe(TFAA)_3$ complex are given in Tables 3 and S2 (supplementary materials), respectively. To increase the assignment accuracy, the vibrational spectra and their assignment of the title complex compared with those of $Fe(AA)_3$ complex, see Tables 4 and S3 (supplementary materials) for vibrational assignment of $Fe(AA)_3$. The internal coordinates achieved from VEDA (.dd2 files) of the both complexes are given in Tables S4–6, supplementary materials.

Fig. 5 shows the solid IR spectra of $Fe(AA)_3$ and $Fe(TFAA)_3$ in the 1800–500 cm^{-1} along with 3100–2800 cm^{-1} regions. The experimental Raman spectra of $Fe(AA)_3$ and $Fe(TFAA)_3$ and theoretical Raman of fac-mer isomers of $Fe(TFAA)_3$ are shown in Figs. 6 and S3 (supplementary material), respectively. The recorded and

Table 3
Shorted vibrational assignments, experimental and calculated wavenumbers along to VEDA's PEDs (in cm^{-1} and %) of $Fe(TFAA)_3$. [a]

$Fe(TFAA)_3$ $M = 6$ [b]										Assignment	
Sym	Theoretical						Experimental			GaussView animation	
	Fac (C_3)			Mer (C_1)[c]							VEDA's PEDs ≥10%
	Fs	I_{IR}	A_R	Fs	I_{IR}	A_R	IR(Solid)	IR(CCl_4)	R(Solid)		
A	3111	1	229	3112	1	112	3091(1)	3089(1)		νCH_α	νCH_α(99)
A				3013	11	71	3004(3)	3001(2)		$\nu_a CH_3$	$\nu_a CH_3$(86)
A	3012	0	81				3004	3001		$\nu_a CH_3$	$\nu_a CH_3$(99)
E				3013	16	74	3004	3001		$\nu_a CH_3$	$\nu_a CH_3$(80)
E	3012	21	67				3004	3001		$\nu_a CH_3$	$\nu_a CH_3$(94)
E				3012	16	74	3004	3001		$\nu_a CH_3$	$\nu_a CH_3$(98)
E	3012	21	67				3004	3001		$\nu_a CH_3$	$\nu_a CH_3$(89)
A	2978	4	123	2978	3	72	2977(3)	2975(2)		$\nu_a CH_3$	$\nu_a CH_3$(88)
A	2921	3	641	2921	2	252	2926(4)	2925(1)		$\nu_s CH_3$	$\nu_s CH_3$(99)
A				1634	17	365	1635(3)	1629(9)	1625(58)	ν_sC-O, ν_sC-C-C	ν_sC-O(61)
A	1634	48	347				1635	1629	1625	ν_sC-O, ν_sC-C-C	ν_sC-O(50)
E				1610	965	30	1610(94)	1610(85)		ν_sC-O, ν_sC-C-C	ν_sC-C-C(53)
E	1610	863	35				1610	1610		ν_sC-O, ν_sC-C-C	ν_sC-O(62)
E	1610	863	35				1610	1610		ν_sC-O, ν_sC-C-C	ν_sC-O(71)
E				1610	811	28	1610	1610		ν_sC-O, ν_sC-C-C	ν_sC-C-C(45)
A	1539	417	5	1538	191	8	1578(25)	1576(38)	1564(51)	ν_aC-C-C, δCH_α	δCH_α(31), ν_aC-C-C(11)
E	1538	76	7	1537	302	5	1526(75)	1526(51)	1529(49)	ν_aC-C-C, δCH_α	ν_aC-C-C(15), δCH_α(34)
A	1466	60	9	1466	73	7	1452(35)	1444(23)	1439(61)	ν_aC-O, $\delta_a CH_3$	$\delta_a CH_3$(64)
A	1451	1	4	1450	6	7	1420(11)			$\delta_a CH_3$	$\delta_a CH_3$(85)
A	1435	220	2	1436	222	1	1364(52)	1363(37)	1368(59)	$\delta_a CH_3$	$\delta_a CH_3$(52)
E				1426	18	6	1364	1363	1368	$\delta_a CH_3$, ν_aC-C-C, ν_aC-O	ν_aC-C-C(22), ν_aC-O(13)
E	1425	76	2				1364	1363	1368	$\delta_a CH_3$, ν_aC-C-C, ν_aC-O	ν_aC-O(49)
E	1425	76	2				1364	1363	1368	$\delta_a CH_3$, ν_aC-C-C, ν_aC-O	ν_aC-C-C(16), ν_aC-O(14)
E				1425	125	10	1364	1363	1368	$\delta_a CH_3$, ν_aC-C-C, ν_aC-O	ν_aC-O(54)
A	1375	73	17	1375	42	12	1351(18)			$\delta_s CH_3$	$\delta_s CH_3$(82)
A	1291	752	67				1288(100)	1299(100)	1283(49)	νC-CF_3, ν_sC-C-C, νC-CH_3	ν_sC-C-C(14), νC-CF_3(10)
A				1290	756	10	1288	1299	1283	νC-CF_3, ν_sC-C-C, νC-CH_3	ν_sC-C-C(33)
E				1286	153	14	1227	1223	1226	$\nu_s CF_3$, δCH_α	$\nu_s CF_3$(46)
E	1287	162	10				1227	1223	1226	$\nu_s CF_3$, δCH_α	$\nu_s CF_3$(29)
E	1287	162	10				1227	1223		$\nu_s CF_3$, δCH_α	$\nu_s CF_3$(27)
E				1286	176	21	1227	1223		$\nu_s CF_3$, δCH_α	$\nu_s CF_3$(41)
A	1221	45	3	1220	19	12	1195(53)	1199(46)	1194(32)	$\nu_s CF_3$, δCH_α	δCH_α(38)
A				1154	98	3	1145(86)	1158(46)		$\delta_a CF_3$, δCH_α	$\delta_a CF_3$(47)
A	1155	47	4				1145	1158		$\delta_a CF_3$, δCH_α	$\delta_a CF_3$(60)
E	1152	400	1				1145	1158		$\delta_a CF_3$, δCH_α	$\delta_a CF_3$(58)
E				1151	390	1	1145	1158		$\delta_a CF_3$, δCH_α	$\delta_a CF_3$(44)
A				1136	182	5	1145	1158		$\delta_s CF_3$, δCH_α	$\delta_s CF_3$(16)
A	1143	436	5				1145	1158		$\delta_s CF_3$, δCH_α	δCH_α(42), $\delta_s CF_3$(11)
E	1134	84	8				1145	1158		$\delta_s CF_3$, δCH_α	$\delta_s CF_3$(50), δCH_α(10)
E				1130	42	12	1145	1158		$\delta_s CF_3$, δCH_α	$\delta_s CF_3$(25)
E	1124	313	9	1128	265	4	1138(86)	1138(43)	1138(39)	$\delta_a CF_3$, δCH_α	$\delta_a CF_3$(58)
A	1033	1	2	1033	3	0	1024(17)	1024(6)	1021(34)	πCH_3	πCH_3(89)
A	958	2	3	958	1	8	949(18)	952(4)	949(30)	δC-C-C, ρCH_3, $\delta_a CF_3$	δC-C-C(13), ρCH_3(13)
E	957	1	3	957	1	1	929(10)	929(4)		δC-C-C, ρCH_3, $\delta_a CF_3$	δC-C-C(27)
A	851	48	2	850	30	1	864(24)	862(10)	861(27)	νC-CH_3, νC-CF_3	νC-CF_3(24), νC-CH_3(10)
E	802	33	1	802	33	1	791(26)		789(26)	γCH_α	γCH_α(78)
E	755	2	3				753(5)			Γ	Γ(86)
E				755	1	1	753			Γ	Γ(56)
A	716	30	20				730(31)		732(41)	$\delta_s CF_3$, ν_sO-Fe-O	$\delta_s CF_3$(35)
A				716	9	15	730		732	$\delta_s CF_3$, ν_sO-Fe-O	ν_sO-Fe-O(16)
E	714	26	5	714	36	4	670(8) #		673(32)	$\delta_s CF_3$, ν_aO-Fe-O	ν_aO-Fe-O(34), $\delta_s CF_3$(16)
E	608	1	2	608	3	1	609(9)			γC-CH_3	γC-CH_3(60)
A	583	0	8	583	1	1	581(48)		596(48)	ν_aO-Fe-O, $\delta_a CF_3$, $\delta OCCH_3$	$\delta_a CF_3$(18)
A	579	63	6	579	27	5	551(11)			ν_aO-Fe-O, δC-C-O, δC-CH_3, $\delta_a CF_3$	ν_aO-Fe-O(33), δC-C-O(15)
A	506	2	1	506	3	1	500(10)		496(59)	$\delta_a CF_3$	$\delta_a CF_3$(67)
A	483	5	10				451(10)		451(95)	$\delta_a CF_3$, ν_aO-Fe-O	ν_aO-Fe-O(25)
				480	18	2	451		451	$\delta_a CF_3$, ν_aO-Fe-O	$\delta_a CF_3$(41)
A	422	14	34	421	29	16	425(33)			ν_sO-Fe-O, δC-C-CH_3, δC-C-CF_3	δC-C-CH_3(34)
E	418	46	2	420	17	8	425			ν_sO-Fe-O, δC-C-CH_3, δC-C-CF_3	ν_sO-Fe-O(39)
E	324	9	2	325	12	4	311(9)		342(25)	δO-Fe-O, δC-CH_3, δC-CF_3	δC-CF_3(58), δO-Fe-O(29)
A	300	0	18	305	32	4	299 (14)		300 (70)	δO-Fe-O, δC-CH_3, δC-CF_3	δC-CH_3(19)
E	294	1	3	294	1	6	287(16)			Γ	Γ(39)
E	281	34	5				276(12)			ν_aO-Fe-O, Δ	ν_aO-Fe-O(17)
E				283	55	6	276			ν_aO-Fe-O, Δ	ν_aO-Fe-O(29)
E				279	19	7	276			ν_aO-Fe-O, Δ	ν_aO-Fe-O(13)
E	281	34	5				276			ν_aO-Fe-O, Δ	ν_aO-Fe-O(25)

(a) Fs, the scaled theoretical frequencies calculated at the B3LYP/6-311++G** level. IIR, IR intensity (in kM/mol); and A_R, Relative calculated Raman intensity (obtained at same level); the relative observed intensities are given in parentheses; ν, stretching; δ, in-plane bending; γ, out-of-plane bending; Δ, in-plane ring deformation; Γ, out-of-plane ring deformation; τ, torsion; ρ, in-plane rocking; π, out-of-plane rocking; # below 700 cm^{-1} recorded with different instrument.
(b) Multiplicity
(c) All symmetry species of mer isomer are *A*.

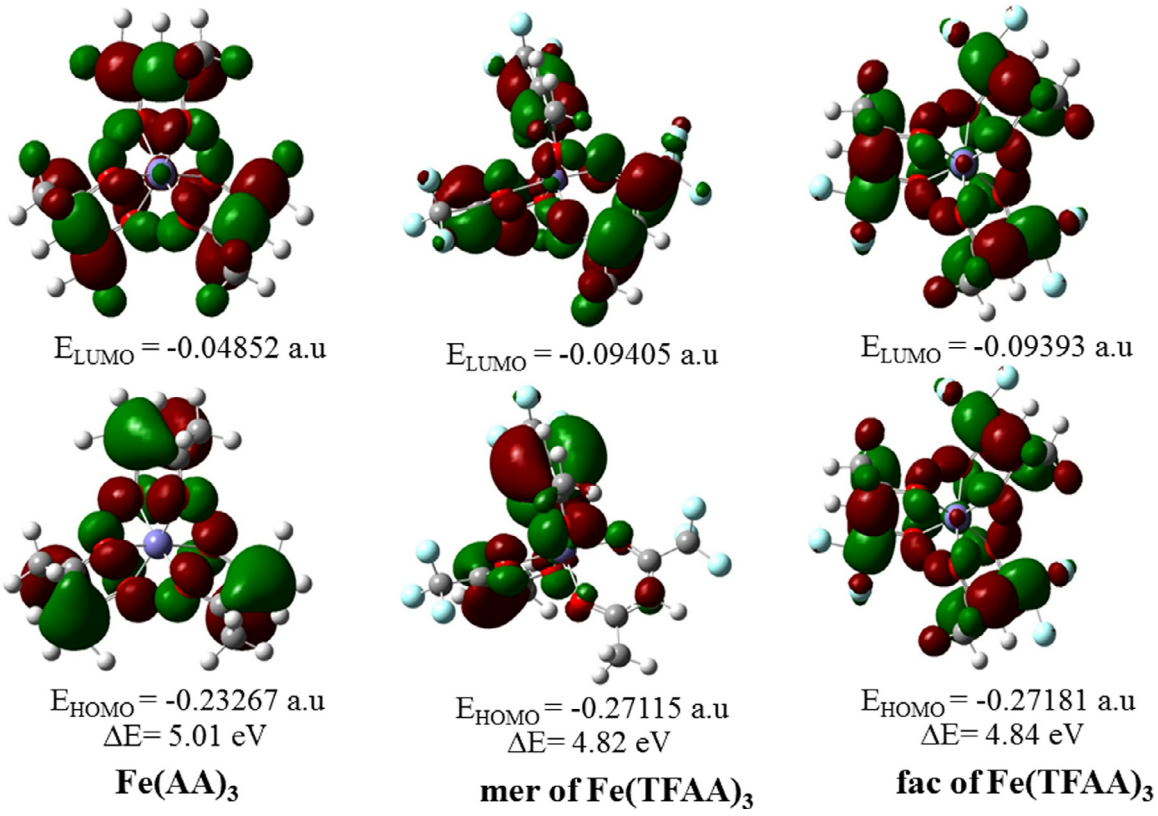

Fig. 3. The calculated HOMO-LUMO energy gaps for the $Fe(AA)_3$, mer and fac of $Fe(TFAA)_3$ complexes.

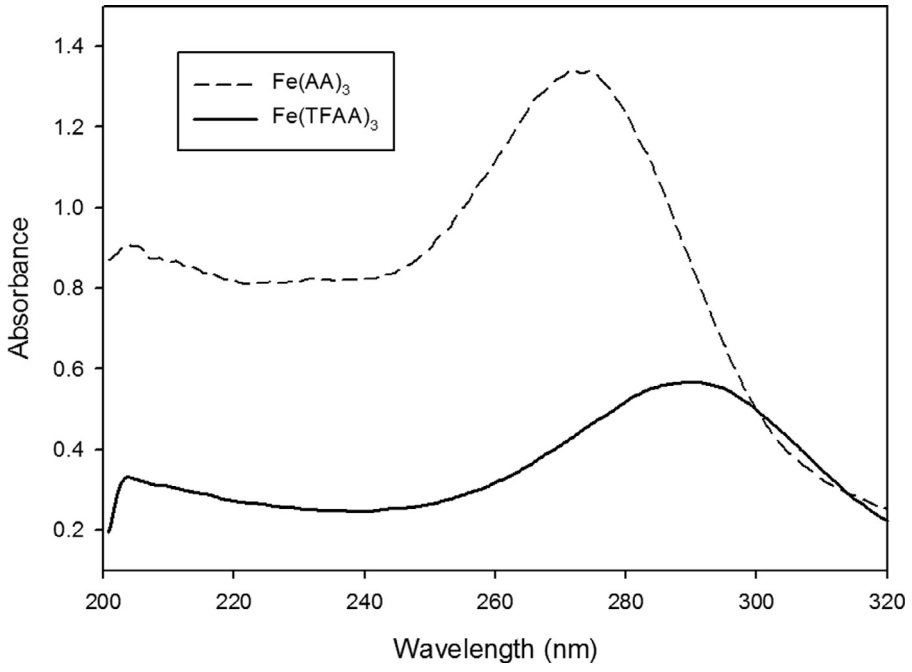

Fig. 4. The experimental UV spectra of $Fe(AA)_3$ and $Fe(TFAA)_3$ complexes in ethanol as solvent.

simulated Far-IR spectra of the $Fe(AA)_3$ along with fac-mer isomers of $Fe(TFAA)_3$ are shown in Fig. 7a and b. In addition, IR spectra of $Fe(TFAA)_3$ in the solid phase and CCl_4 solution are compared in Fig. S4 (supplementary material).

Since the theoretical wavenumbers are higher than the experimental ones, so the appropriate scales, 0.9609 for upper 2000 cm^{-1} and 0.9859 for below 2000 cm^{-1} regions, are used to theoretical numbers [33]. For this purpose the correlation between theoretical and experimental frequencies of both complexes are shown in Fig. 8a and b. These figures clarified those *R* square values, 0.9998 and 0.9991 from unscaled theoretical frequencies increased to 0.9999 and 0.9993 in effect of scaled theoretical frequencies for Fe(TFAA) and $Fe(AA)_3$, respectively.

3.2.2.1. 3000 cm^{-1} region. In this region, vibrational stretching of CH_α and methyl groups can be observed. According to Table 3, in

Table 4
Shorted vibrational assignments, experimental, and calculated wavenumbers along to VEDA's PEDs (in cm^{-1} and %) of $Fe(AA)_3$. [a]

Sym.	$Fe(AA)_3$								
	Theoretical			Experimental		Assignment			
	Fs	I_{IR}	A_R	IR(Solid)	R(Solid)	GaussView animation	VEDA's PEDs≥10%	Ref [41].	Ref [66].
A_1	3078	0	232		3085(7)	$\nu_s CH_\alpha$	$\nu_s CH_\alpha$(97)		
E	3078	15	71	3081(3)	3085	$\nu_a CH_\alpha$	$\nu_a CH_\alpha$(97)	ν(CH)	
A_1	3003	0	137		3006(5)	$\nu_a CH_3$	$\nu_a CH_3$(92)		
E	3003	57	159	2998(6)	3006	$\nu_a CH_3$	$\nu_a CH_3$(87)		
E	3003	57	159	2998	3006	$\nu_a CH_3$	$\nu_a CH_3$(87)		
E	2974	14	4	2961(5)	2960(8)	$\nu_a CH_3$	$\nu_a CH_3$(92)		
A_1	2974	0	248		2960	$\nu_a CH_3$	$\nu_a CH_3$(98)		
A_1	2917	0	1273		2928(32)	$\nu_s CH_3$	$\nu_s CH_3$(78)		
E	2917	7	30	2919(7)	2928	$\nu_s CH_3$	$\nu_s CH_3$(91)	$\nu(CH_3)$	
E	2917	7	30	2919	2928	$\nu_s CH_3$	$\nu_s CH_3$(90)	$\nu(CH_3)$	
A_1	1612	0	278	1608(7)	1608(100)	ν_sC-O, ν_sC-C-C, δCH_3	ν_sC-O(63)		
E	1584	954	22	1579(100)	1587(41)	ν_sC-O, ν_sC-C-C, δCH_3	ν_sC-O(70)	ν(C=O), ν(C=C)	ν(C=C)
A_2	1530	766	0	1525(70)		ν_aC-C, ν_aC-CH_3, δCH_α	ν_aC-C(44), δCH_α(15)	ν(C=C), δ(C=CH)	ν(C=O)
E	1458	135	8	1442(15)		$\delta_a CH_3$	$\delta_a CH_3$(85)		ν(C=O), δ(CH)
E	1458	135	8	1442		$\delta_a CH_3$	$\delta_a CH_3$(78)		ν(C=O), δ(CH)
A_2	1452	12	0	1421(18)		$\delta_a CH_3$	$\delta_a CH_3$(89)	$\delta(CH_3)$	
E	1452	17	15	1421	1428(8)	$\delta_a CH_3$	$\delta_a CH_3$(75)	$\delta(CH_3)$	
A_2	1407	572	0	1390(34)		ν_aC-O, $\delta_a CH_3$, ν_aC-C-C,	ν_aC-C-C(52),	ν(C=O), ν(C=C)	δaCH_3
E	1391	134	0	1371(33)		ν_aC-C-C, ν_aC-O, $\delta_a CH_3$	ν_aC-C-C(59), $\delta_a CH_3$(11)	ν(C=O), ν(C=C)	
A_1	1376	0	32		1370(24)	$\delta_s CH_3$	$\delta_s CH_3$(82)	$\delta(CH_3)$	$\delta_s CH_3$
E	1375	15	11	1358(45)	1370	$\delta_s CH_3$	$\delta_s CH_3$(84)	$\delta(CH_3)$	$\delta_s CH_3$
A_1	1276	0	31		1278(32)	ν_sC-C-C, ν_sC-CH_3	ν_sC-C-C(50)	ν(C=C), ν(C-CH_3)	
E	1270	127	7	1273(53)	1278	ν_sC-CH_3, ν_sC-C-C	ν_sC-C-C(29),ν_sC-CH_3(13)	ν(C=C), ν(C-CH_3)	ν(C=C), ν(C-CH_3)
E	1270	127	7	1273	1278	ν_sC-C-C, ν_sC-CH_3	ν_sC-C-C(50)	ν(C=C), ν(C-CH_3)	ν(C=C), ν(C-CH_3)
A_2	1199	35	0	1189(5)		$\delta_s CH_\alpha$, ν_sC-O	$\delta_s CH_\alpha$(47), ν_sC-O(10)	δ(C=CH), ν(C=O)	δsCH
E	1197	3	18	1189	1186(11)	$\delta_a CH_\alpha$, ν_sC-O	$\delta_a CH_\alpha$(57), ν_sC-O(13)	δ(C=CH), ν(C=O)	δsCH
A_1	1040	0	2		1033(12)	πCH_3	πCH_3(74)		
E	1040	0	0			πCH_3	πCH_3(80)		
E	1040	0	0			πCH_3	πCH_3(78)		
A_1	1029	0	1			ρCH_3, ν_sO-Fe-O	ρCH_3(25), ν_sO-Fe-O(12)		
E	1027	14	0	1024(26)	1023(14)	πCH_3	πCH_3(82)	ρr(CH_3)	ρCH_3
E	1026	37	0	1018(17)		ρCH_3, ν_sO-Fe-O	ρCH_3(45), ν_sO-Fe-O(27)	ρr(CH_3), ν(C=O), πring	
A_2	1018	8	0	1009(20)	1010(9)	ρCH_3, ν_sO-Fe-O	ρCH_3(81)		
A_1	948	0	13	942(9)	940(14)	ρCH_3, δC-C-C	ρCH_3(19)		
A_2	928	32	0	929(28)		ν_aC-CH_3, Δ	ν_aC-CH_3(82)	ν(C-CH_3)	ν(C-CH_3), νC-O
				801(10)		Combination	Combination		γC-H
E	773	21	4	770(18)	789(8)	γCH_α	γCH_α(91)	π(C-H)	
E	664	7	0	666(25) #		γC-CH_3, Γ	γC-CH_3(58), Γ(12)	πring, Mixed	πring, ν(M-O)
A_1	655	0	12		669(14)	ν_sO-Fe-O,ν_sC-CH_3, δC-C-O	ν_sC-CH_3(25), δC-C-O(18)	ν(C-CH_3),ν(Fe-O)	
E	650	38	6	653(5)	669	ν_sO-Fe-O, ν_sC-CH_3, δC-C-O	δC-C-O(37), ν_sO-Fe-O(33)	ν(C-CH_3),ν(Fe-O)	δ(C-CH_3), ν(M-O)
A_1	558	0	4		563(11)	γ_sC-CH_3, γC-C-O	γC-C-O(76)		
A_2	539	38	0	559(9)		ν_aO−Fe−O, δC-CH_3	δC-CH_3(67)	δ(O=C-CH_3)	
E	531	13	1	548(10)	541(7)	ν_aOFe-O, δC-C-O, δC-CH_3	δC-C-O(63)	δ(O=C-CH_3)	
A_1	430	0	74		446(64)	ν_sO-Fe-O, δC-C-C, δC-CH_3	δC-C-C(45), δC-CH_3(10)	ν(Fe-O)	
E	422	97	3	433(60)	433(17)	ν_sO-Fe-O, δC-C-C, δC-CH_3	δC-C-C(51)		ν(M-O)
A_2	409	18	0	414(14)		δC-CH_3, δC-C-O	δC-C-O(58)	δ(C=C-CH_3, O=C=C)	Γ
E	405	13	2	407(19)	404(7)	δC-CH_3, δC-C-O	δC-C-O(66), δC-CH_3(10)	δ(C=C-CH_3, O=C=C)	
E	295	76	7	298(28)	298(21)	ν_aO-Fe-O, Δ	ν_aO-Fe-O(37), Δ(22)	ν(Fe-O), δ(O-Fe-O)	ν(M-O)
E	245	2	2		253(12)	δO-Fe-O, Δ	Δ(57)	δ(C=O-Fe, CH_3-C=C)	δC-CH3
E	195	3	1	205(16)	207(18)	Γ	Γ(56)		Ring def
A_1	164	0	10		170(11)	$\tau CCOCH_3$	$\tau CCOCH_3$(49)		

[a] See footnote Table 3.

IR spectra of $Fe(TFAA)_3$ in the solid and CCl_4, the very weak band at about 3090 cm^{-1} is assigned to the CH_α stretching. The corresponding band in $Fe(AA)_3$, $Cr(AA)_3$, and $Al(TFAA)_3$ as trivalent complexes, reported at 3081, 3083, and 3122 cm^{-1}, respectively [3,33]. Diaz-Acosta et al. [41] also considered the band at 3088 cm^{-1} as CH_α stretching vibration of $Fe(AA)_3$. This normal mode in the Raman spectrum was observed at 3085 cm^{-1}, see Table 4. The VEDA's PEDs of CHα str. are upper than 90%.

The IR spectrum of $Fe(TFAA)_3$ shows three bands at 3004, 2977, and 2926 cm^{-1}, which according to theoretical results and comparison with the corresponding bands of $Cr(AA)_3$ and $Al(TFAA)_3$ assigned to the asymmetric and symmetric stretching of CH_3 groups. Although in asymmetric stretching of CH_3 normal modes the PED values for fac and mer of $Fe(TFAA)_3$ have difference. The corresponding bands for $Fe(AA)_3$ observed at 2998 (3006), 2961 (2960), and 2919 (2928) cm^{-1}. The values in parentheses are Raman bands.

3.2.2.2. 1700–1000 cm^{-1} region. In addition to the CF_3 stretching, we expect to observe some bands due to the CH_3 and CF_3 deformations, C−CH_3 and C−CF_3 stretching, and CH in-plane bending vibrations in this region. The IR spectra of $Fe(TFAA)_3$ in solid and CCl_4 solution show a very strong band at 1610 cm^{-1}, that according to our calculations assigned to the C−O coupled with C−C−C symmetric stretching vibrations. VEDA's PEDs shows that for the mentioned mode the contributions of fac and mer of $Fe(TFAA)_3$ about 10% are changed. This Raman band appears as a high-intensity band at 1625 cm^{-1}. In the solid IR spectrum of $Fe(AA)_3$ this band appears at 1579 cm^{-1}, that its experimental and theoretical red shift can be due to coupling with CH_3 bend-

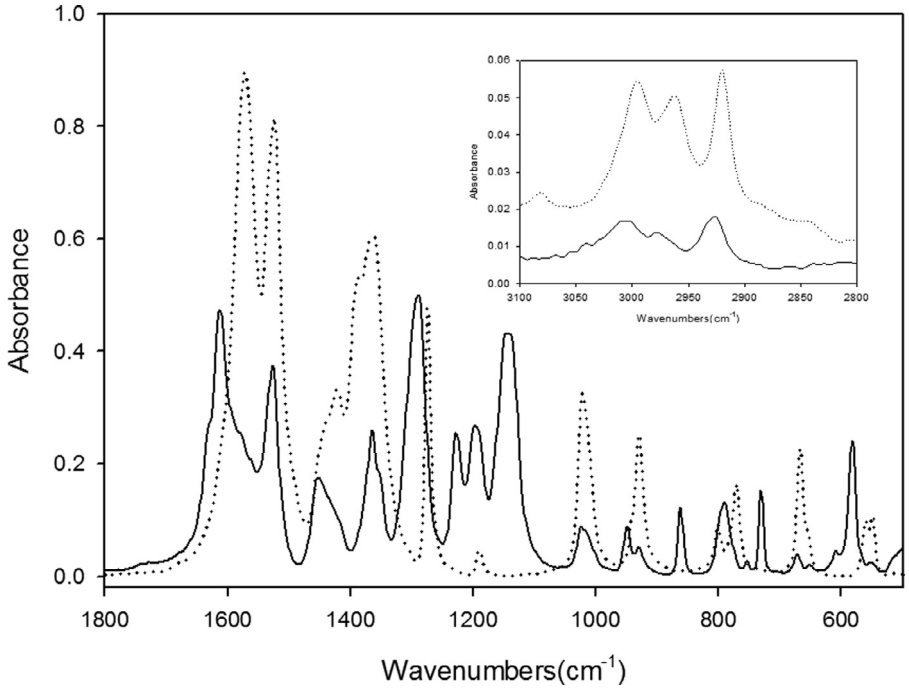

Fig. 5. The recorded infrared spectra of $Fe(TFAA)_3$ (−) and $Fe(AA)_3$ (.....) complexes in solid phase in the 1800–500 and 3100–2800 cm^{-1} region.

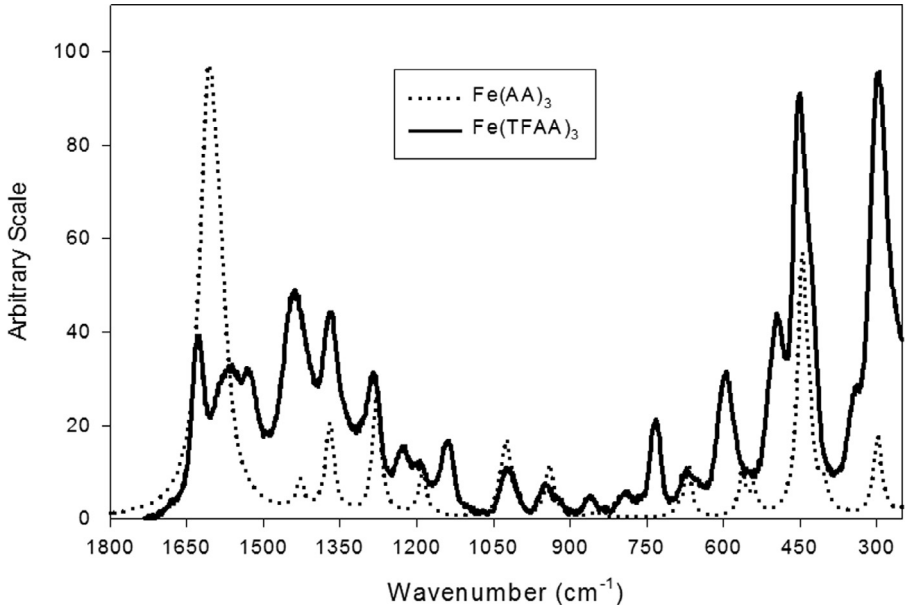

Fig. 6. The recorded Raman spectra of $Fe(TFAA)_3$ (−) and $Fe(AA)_3$ (.....) complexes in solid phase in the 1800–250 cm^{-1} region.

ing and electron-withdrawing effect of CF_3. This band in $Cr(AA)_3$ and $Al(TFAA)_3$ were reported at 1575 and 1625 cm^{-1}, respectively [3,33]. The 1578 and 1526 cm^{-1} bands in the IR spectrum of $Fe(TFAA)_3$ were assigned to the asymmetric C–C–C stretching which according to PEDs coupled to the in-plane bending mode, δCH_α. The corresponding Raman bands were observed at 1564 and 1529 cm^{-1}, respectively. These bands were assigned to the C=O and C=C stretching coupled to the CH in-plane bending by Diaz-Acosta et al. [41], which is somewhat in agreement with our assignment.

According to the calculated results and comparing with the vibrational assignment of 1,1,1-trifluoro-2,4-pentanedione, TFAA [59], the medium-intensity IR and Raman bands of $Fe(TFAA)_3$ at 1452 and 1439 cm^{-1} assigned to the $\nu_a C{-}O$ coupled to $\delta_a CH_3$. The corresponding band in $Al(TFAA)_3$ splitted as two bands, at 1490 and 1458 cm^{-1} [3]. In $Fe(AA)_3$ the mentioned IR band observed at 1390 cm^{-1}, as shoulder bands. Diaz-Acosta et al. also considered this band as $\nu C{=}O$ vibrations for $Fe(AA)_3$ [41].

The $\delta_a CH_3$ and $\delta_s CH_3$ vibrations, asymmetric and symmetric deformation of the methyl group, in the IR spectrum of $Fe(TFAA)_3$ appeared at 1420, 1364, and 1351 cm^{-1}, respectively. These bands in $Fe(AA)_3$, $Al(TFAA)_3$, and $Cr(AA)_3$ complexes observed at 1421 (1358), 1419 (1368), and 1423 (1367), that the values in parenthesis are $\delta_s CH_3$ of the mentioned molecules [3,33]. The corresponding Raman bands of $Fe(AA)_3$ for the mentioned asymmetric and symmetric deformation are 1428 and 1370 cm^{-1}, respectively.

The IR spectrum of $Fe(TFAA)_3$ complex in the solid phase indicates a strong-intensity band at 1288 cm^{-1}, which is assigned to

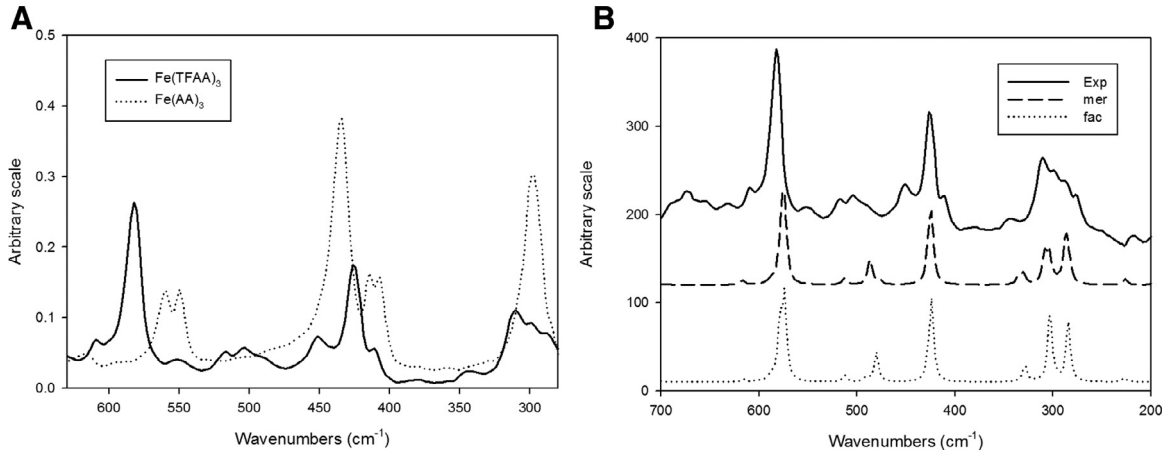

Fig. 7. (a) The recorded Far IR spectra of the $Fe(TFAA)_3$ and $Fe(AA)_3$ complexes in solid phase in the 700–250 cm^{-1} region. (b) Comparing of simulated Far IR spectra of $Fe(TFAA)_3$, fac and mer, and its experimental in the 700–200 cm^{-1} region.

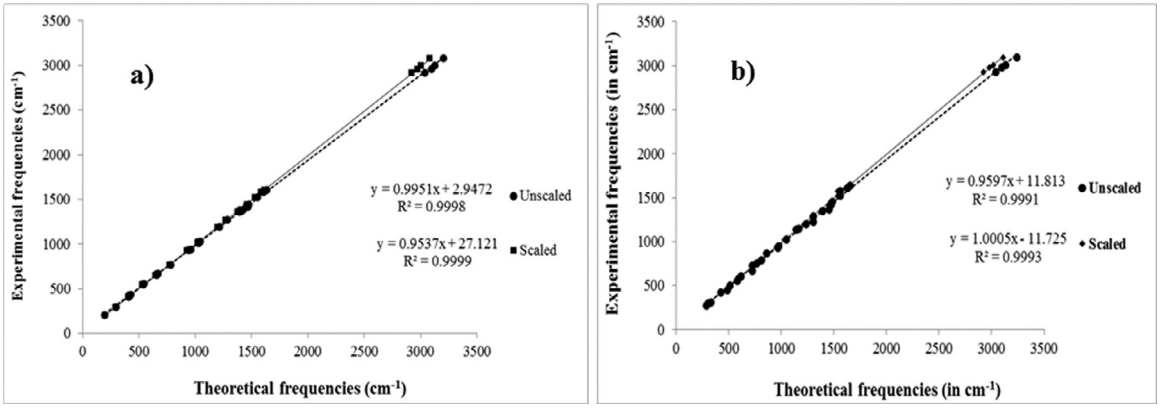

Fig. 8. (a) The correlation between theoretical and experimental frequencies of $Fe(TFAA)_3$ and for $Fe(AA)_3$ in (b).

$\nu C-CF_3$,$\nu_s C-C-C$,$\nu C-CH_3$ for fac isomer, while upon PED of mer isomer there is not any coupling. This band in TFAA appeared at 1284 cm^{-1}, with about the same intensity but with a broader band width, which is due to coupling with δOH. The mentioned band in $Al(TFAA)_3$, $Fe(AA)_3$, and $Cr(AA)_3$ complexes observed at 1306, 1273, and 1278 cm^{-1} [3,33]. This vibrational frequency in the Raman spectrum of $Fe(AA)_3$ and $Fe(TFAA)_3$ was observed at 1278 and 1283 cm^{-1}, respectively.

Similar to $Al(TFAA)_3$ [3], two strong intensity IR bands at 1227 and 1195 cm^{-1} of $Fe(TFAA)_3$ complex assigned to the $\nu_s CF_3$ stretching vibration, which coupled to δCH_α. The contributions of $\nu_s CF_3$ stretching mode in mer isomer about 15% more than that fac isomer. The corresponding Raman bands appeared at 1226 and 1194 cm^{-1}. The δCF_3 movement for this complex coupled with δCH_α and observed at 1145 and 1138 cm^{-1} as strong intensity IR bands. The IR weak intensity band of $Fe(AA)_3$ at 1189 cm^{-1} assigned to δCH_α, $\nu_s C-O$.

3.2.2.3. Below 1000 cm^{-1} region. We expect to observe Fe–O, C–CF_3, and C–CH_3 stretching, in-plane bending of CF_3 group, out-of-plane bending of CH_α, and in- and out-of-plane deformations of chelated ring movements in this region. Upon theoretical results of $Fe(TFAA)_3$, the IR weak intensity bands at 949 and 929 cm^{-1} assigned to the C–C–C in-plane bending coupled to the CH_3 rocking and $\delta_a CF_3$. This band in $Fe(AA)_3$, $Cr(AA)_3$, and $Al(TFAA)_3$ complexes reported at 942, 939, and 957 cm^{-1} [3,33]. According to the animation of GaussView, the splitting in $Fe(TFAA)_3$ maybe due to coupling with $\delta_a CF_3$.

The medium intensity IR and Raman band in $Fe(TFAA)_3$ at about 864 cm^{-1} assigned to the C–CF_3 stretching mode coupled to the C–CH_3 stretching motion. This band was indicated in TFAA and $Al(TFAA)_3$ at 858 and 868 cm^{-1}, respectively [3,59]. The CH out-of-plane bending, γCH_α, of the titled complex was observed at 791 cm^{-1} as a medium intensity IR band. The corresponding band in $Fe(AA)_3$ was observed at 770 cm^{-1}, which agrees with the reported assignment by Diaz-Acosta et al. [41]. This red shift agrees with calculated wavenumbers too, see Tables 4 and S3.

According to calculated results, the IR band at 753 cm^{-1} in the titled complex assigned to the out-of-plane deformation of the chelated ring, Γ. The contribution of the mentioned normal mode for mer about 30% lower respect to the fac isomer. While the mentioned band in $Al(TFAA)_3$ split as two, medium and weak intensity bands, at 785 and 758 cm^{-1}, respectively. This band in $Fe(AA)_3$ and $Cr(AA)_3$ shifted to about 666 cm^{-1}, which is due to the coupling with $\gamma C-CH_3$ [3,33]. This shift agrees with the calculation wavenumbers. Nakamoto et al. [66,67] assigned the 654 cm^{-1} band to the deformation vibration of $Fe(AA)_3$.

Afzali et al. [3] assigned the IR band at 735 cm^{-1} of $Al(TFAA)_3$ to symmetric CF_3 bending coupled with symmetric Al–O stretching. This band in IR and Raman spectra of $Fe(TFAA)_3$ complex appeared as two bands at about 730 and 670 cm^{-1}. According to GaussView visualization, they coupled with $\nu_s O-Fe-O$ and

ν_aO−Fe−O movement, respectively, while upon VEDA's PEDs the first band is $\delta_s CF_3$ for fac and ν_sO−Fe−O for mer isomer. The mentioned band has not been observed in $Fe(AA)_3$ and $Cr(AA)_3$ complexes.

By increasing the metal-ligand, M−L, strength, the frequency of the O−M stretching is expected to increases. The Fe−O asymmetrical stretching band in $Fe(AA)_3$ was observed as two medium intensity bands at 559 and 548 cm^{-1} (average 554 cm^{-1}). These vibrational band frequencies in $Fe(TFAA)_3$ appear at 581 and 551 cm^{-1}, as a strong and a weak intensity band, respectively. The difference in their intensities is due to different contributions of coupling with other vibrational modes. According to the animation of GaussView, the contributions of $\delta_a CF_3$ and δC−C−O in the high-intensity band are lower and higher than that in the low-intensity band, respectively. Also, the symmetric Fe−O stretching, ν_sFe−O, vibrational band in $Fe(TFAA)_3$ and $Fe(AA)_3$ are observed at 425 and 433 cm^{-1}, respectively. This band in $Fe(AA)_3$ assigned to ν_sFe−O, δCCC, δCCH_3, while in $Fe(TFAA)_3$ assign to ν_sFe−O, $\delta CCCH_3$, $\delta CCCF_3$. In addition to M−L strength, the shifted of these bands in $Fe(TFAA)_3$ in comparison to $Fe(AA)_3$ is due to their different couplings.

Nakamoto et al. [66,67] assigned the 298 cm^{-1} band to the Fe−O stretching vibration of $Fe(AA)_3$. According to our calculations, this band is assigned to the asymmetric O−Fe−O stretching vibration coupled to the ring deformation. According to our calculation results, in the Far-IR of $Fe(TFAA)_3$, the medium intensity bands in the 315–270 cm^{-1} region are assigned to the different vibrational modes of the molecule, such as δO−Fe−O, δC-CH_3, δC−CF_3, and out-of-plane and in-plane deformation of the chelated ring. The ν_aFe−O vibration is coupled with in-plane deformation of the chelated ring.

The theoretical and experimental Far-IR spectra of $Fe(TFAA)_3$ in the 700–250 cm^{-1} region are compared in Fig. 7a and b. For comparison and the best assignment, the recorded Far-IR spectrum of $Fe(AA)_3$ is also shown in Fig. 7a. According to Fig. 7b and Table 3, since there is no difference in the calculated frequencies and their intensities of mer and fac isomers, so the vibrational spectroscopy cannot be used to determine the type of isomer in the sample. Therefore, the possibility of two isomers in the sample is reasonable, which agrees with their molecular structures and relative energies.

4. Conclusion

The molecular structure, Fe−O bond strength, UV, and vibrational spectra of $Fe(TFAA)_3$ complex have been studied and compared with the corresponding parameters for $Fe(AA)_3$. Comparing the theoretical results (structural parameters and AIM results) and the experimental data (UV and vibrational spectra) of $Fe(TFAA)_3$with $Fe(AA)_3$ suggests that the metal-ligand bond strength in $Fe(TFAA)_3$ is almost the same as that in $Fe(AA)_3$. In addition, the relative energies show that both isomers of $Fe(TFAA)_3$ are present in the sample. Since there is no important difference between the simulated and experimental vibrational spectra of both $Fe(TFAA)_3$ isomers, it is not possible to use vibrational spectroscopy to distinguish coexisting of both isomers. By the aid of DFT calculations and the experimental vibrational spectra of $Fe(TFAA)_3$, $Fe(AA)_3$, and the accessible similar complexes data, a complete vibrational assignment along to PEDs of the titled complexes was accomplished. Since the symmetry and asymmetry Fe−O stretching in $Fe(TFAA)_3$ and $Fe(AA)_3$coupled with different movement, so the vibrational spectroscopy cannot compare the Fe−O bond strength of these molecules.

Declaration of Competing Interest

The authors declare that they have no known competing financial interests or personal relationships that could have appeared to influence the work reported in this paper.

CRediT authorship contribution statement

Farzad Gandomi: Methodology, Formal analysis, Investigation, Writing – original draft. **Mohammad Vakili:** Conceptualization, Supervision, Writing – review & editing. **Reza Takjoo:** Writing – review & editing. **Sayyed Faramarz Tayyari:** Supervision, Writing – review & editing.

Acknowledgments

The authors would like to express their sincere thanks and appreciation to Ferdowsi University of Mashhad for the financial support during this research.

Funding

The authors did not receive support from any organization for the submitted work.

Consent to participate

All authors agreed to participate in this research.

Supplementary materials

Additional supporting information can be found in Tables S1–6 and Figs. S1–4 in supplementary materials.

Supplementary material associated with this article can be found, in the online version, at doi:10.1016/j.molstruc.2021.131347.

References

[1] A.W. Maverick, M.L. Ivie, J.H. Waggenspack, F.R. Fronczek, Intramolecular binding of nitrogen bases to a cofacial binuclear copper (II) complex, Inorg. Chem. 29 (1990) 2403–2409, doi:10.1021/ic00338a005.
[2] H. Fakheri, S.F. Tayyari, M.M. Heravi, A. Morsali, Low frequency vibrational spectra and the nature of metal-oxygen bond of alkaline earth metal acetylacetonates, J. Mol. Struct. 1150 (2017) 340–348, doi:10.1016/j.molstruc.2017.08.041.
[3] R. Afzali, M. Vakili, E. Boluri, S.F. Tayyari, A.R. Nekoei, M. Hakimi-Tabar, V. Darugar, Structure, isomerism, and vibrational assignment of aluminumtrifluoroacetylacetonate. An experimental and theoretical study, Spectrochim. Acta A 190 (2018) 15–22, doi:10.1016/j.saa.2017.08.075.
[4] B.Q. Ma, S. Gao, Z.M. Wang, C.S. Liao, C.H. Yan, G.X. Xu, Synthesis and structure of bis (dibenzoylmethane) copper (II), J. Chem. Cryst. 29 (1999) 793–796, doi:10.1023/A:1009543703278.
[5] V.D. Pillai, V.M. Shinde, Synergistic extraction of copper (II), cobalt (II) and nickel (II) with trifluoroacetylacetoneandpyridine, Indian J. Chem. 34A (1995) 407–409 http://nopr.niscair.res.in/handle/123456789/40023.
[6] V.D. Pillai, V.M. Shinde, Synergistic extraction of uranium (VI) and iron (III) using trifluoroacetylacetone and pyridine, Indian, J. Chem. 35A (1996) 906–908 http://nopr.niscair.res.in/handle/123456789/41457.
[7] R. Liu, P.H. Van Rooyen, J. Conradie, Geometrical isomers of tris (β-diketonato) metal (III) complexes for M= Cr or Co: synthesis, X-ray structures and DFT study, Inorg. Chim. Acta 447 (2016) 59–65, doi:10.1016/j.ica.2016.03.019.
[8] M.L. Hu, Z.M. Jin, Q. Miao, L.P. Fang, Crystal structure of tris (acetylacetonato) iron (III), $C_{15}H_{21}O_6Fe$, at 20 K, Z. Kristallogr. New Cryst. Struct. 216 (2001) 597598, doi:10.1524/ncrs.2001.216.14.631.
[9] C.E. Pfluger, P.S. Haradem, Coordination sphere geometry of tris (acetylacetonato) metal (II) complexes: the crystal and molecular structure of tris (1,1,1,5,5,5-hexafluoroacetylacetonato) iron (III), Inorg. Chim. Acta 69 (1983) 141–146, doi:10.1016/S0020-1693(00)83564-1.
[10] J. Iball, C.H. Morgan, A refinement of the crystal structure of ferricacetylacetonate, Acta Crystallogr. 23 (1967) 239–244, doi:10.1107/S0365110X67002531.
[11] S.A. Gromilov, V.I. Lisoivan, I.A. Baidina, S.V. Borisov, X-ray diffraction study of trivalent metal trifluoroacetylacetonates, J. Struct. Chem. 31 (1991) 800–802, doi:10.1007/BF00752563.
[12] R. Gostynski, P.H. Van Rooyen, J. Conradie, X-ray diffraction and QTAIM calculations of the non-covalent intermolecular fluorine-fluorine interactions in tris (trifluoroacetylacetonato)-manganese (III), J. Mol. Struct. 1201 (2020) 127119, doi:10.1016/j.molstruc.2019.127119.

[13] H. Katô, J. Gohda, Magnetic circular dichroism of $Cu(acac)_2$, $Fe(acac)_3$, and $Co(acac)_3$, Bull. Chem. Soc. Jpn. 46 (1973) 636–637, doi:10.1246/bcsj.46.636.

[14] M.M. Conradie, P.H. Van Rooyen, J. Conradie, Crystal and electronic structures of tris [4, 4, 4-Trifluoro-1-(2-X)-1, 3-butanedionato] iron (III) isomers (X= thienyl or furyl): an X-ray and computational study, J. Mol. Struct. 1053 (2013) 134–140, doi:10.1016/j.molstruc.2013.09.014.

[15] M.M. Conradie, P.H. Van Rooyen, J. Conradie, X-ray and electronic structure of tris (benzoylacetonato-κ^2O,O′) iron (III), J. Mol. Struct. 1123 (2016) 199–205, doi:10.1016/j.molstruc.2016.06.027.

[16] M.M. Conradie, J. Conradie, Electrochemical behavior of Tris (β-diketonato) iron (III) complexes: a DFT and experimental study, Electrochim. Acta 152 (2015) 512–519, doi:10.1016/j.electacta.2014.11.128.

[17] N. Tachikawa, R. Haruyama, K. Yoshii, N. Serizawa, Y. Katayama, Redox reaction of tris (acetylacetonato) iron (III) complex in an amide-type ionic liquid, Electrochemistry 86 (2018) 32–34, doi:10.5796/electrochemistry.17-00080.

[18] A.L. Willis, Z. Chen, J. He, Y. Zhu, N.J. Turro, S. O'Brien, Metal acetylacetonates as general precursors for the synthesis of early transition metal oxide nanomaterials, J. Nanomater. (2007) 2007, doi:10.1155/2007/14858.

[19] M. Vakili, S.F. Tayyari, M. Hakimi-Tabar, A.R. Nekoei, S. Kadkhodaei, Structure and vibrational assignment of bis (benzoylacetonato) copper (II), J. Mol. Struct. 1058 (2014) 308–317, doi:10.1016/j.molstruc.2013.11.018.

[20] A.R. Nekoei, M. Vakili, M. Hakimi-Tabar, S.F. Tayyari, R. Afzali, H.G. Kjaergaard, Theoretical study, and infrared and Raman spectra of copper (II) chelated complex with dibenzoylmethane, Spectrochim. Acta A 128 (2014) 272–279, doi:10.1016/j.saa.2014.02.097.

[21] M. Vakili, S.F. Tayyari, R. Afzali, Conformation, molecular structure, and vibrational assignment of bis (2, 2, 6, 6-tetramethylheptane-3, 5-dionato) copper (II), Spectrochim. Acta A 136 (2015) 1827–1833, doi:10.1016/j.saa.2014.10.092.

[22] S. Soltani-Ghockhaneh, M. Vakili, S.F. Tayyari, A.R. Berenji, V. Darugar, Conformation, molecular structure, and vibrational assignment of bis (3, 5-heptanedionato) copper (II), J. Mol. Struct. 1197 (2019) 443–449, doi:10.1016/j.molstruc.2019.07.076.

[23] F. Gandomi, M. Vakili, S.F. Tayyari, Vibrational spectra, normal coordinate analysis, and conformation of bis (a-cyanoacetylacetonato) Cu (II), J. Mol. Struct. 1118 (2016) 68–74, doi:10.1016/j.molstruc.2016.03.101.

[24] S.F. Tayyari, T. Bakhshi, S.J. Mahdizadeh, S. Mehrani, R.E. Sammelson, Structure and vibrational assignment of magnesium acetylacetonate: a density functional theoretical study, J. Mol. Struct. 938 (2009) 76–81, doi:10.1016/j.molstruc.2009.09.006.

[25] S.F. Tayyari, T. Bakhshi, M. Ebrahimi, R.E. Sammelson, Structure and vibrational assignment of beryllium acetylacetonate, Spectrochim. Acta A 73 (2009) 342–347, doi:10.1016/j.saa.2009.02.027.

[26] S. Shibata, M. Ohta, R. Tani, Molecular structure of bis (acetylacetonato) nickel (II) in the gas phase as determined from electron diffraction data, J. Mol. Struct. 73 (1981) 119–124, doi:10.1016/0022-2860(81)85054-5.

[27] S. Shibata, M. Ohta, Molecular structure of bis (acetylacetonato) zinc (II) in the gas phase as determined from electron diffraction data, J. Mol. Struct. 77 (1981) 265–270, doi:10.1016/0022-2860(81)80070-1.

[28] S. Seyedkatouli, M. Vakili, S.F. Tayyari, R. Afzali, Molecular structure, spectroscopic studies, and copperoxygen bond strength of α-methyl and α-ethyl derivatives of copper (II) acetylacetonate: experimental and theoretical approach, J. Mol. Struct. 1160 (2018) 107–116, doi:10.1016/j.molstruc.2018.01.075.

[29] S. Seyedkatouli, M. Vakili, S.F. Tayyari, Vibrational assignment and the effect ofα-methyl and ethyl substitutions on the Cu−O strength in bis-(3-alkylpentane-2, 4-dionato) copper (II); an experimental and DFT study, in: Proceeding of the 14th International Conference on Molecular Spectroscopy, 2017 September).

[30] S.F. Tayyari, M. Jamialahmadi, M. Ghafari, Z. Moosavi-Tekieh, Vibrational assignments and structure of bis (3-amino-1-phenyl-2-buten-1-onato) copper (II) complex, J. Mol. Struct. 1111 (2016) 25–32, doi:10.1016/j.molstruc.2016.01.066.

[31] R. Afzali, M. Vakili, V. Darugar, Isomerism, conformation, and structure of Bis (4, 4-dimethyl-1-phenylpentane-1, 3-dionato) copper (II); a theoretical and spectroscopy approach, J. Mol. Struct. 1227 (2021) 129711, doi:10.1016/j.molstruc.2020.129711.

[32] K. Vus, M. Girych, V. Trusova, G. Gorbenko, A. Kurutos, A. Vasilev, Cyanine dyes derived inhibition of insulin fibrillization, J. Mol. Liq. 276 (2019) 541–552, doi:10.1016/j.molliq.2018.11.149.

[33] F. Dolati, M. Vakili, A. Ebrahimi, S.F. Tayyari, Vibrational spectra of tris (acetylacetonato) chromium(III), J. Mol. Struct. 1099 (2015) 340–347, doi:10.1016/j.molstruc.2015.05.058.

[34] S. Carlotto, L. Floreano, A. Cossaro, M. Dominguez, M. Rancan, M. Sambi, M. Casarin, The electronic properties of three popular high spin complexes [TM $(acac)_3$, TM= Cr, Mn, and Fe] revisited: an experimental and theoretical study, Phys. Chem. Chem. Phys. 19 (2017) 24840–24854, doi:10.1039/C7CP04461E.

[35] K. Sugisaki, K. Toyota, K. Sato, D. Shiomi, T. Takui, Behaviour of DFT-based approaches to the spin-orbit term of zero-field splitting tensors: a case study of metallocomplexes, $M^{III}(acac)_3$ (M= V, Cr, Mn, Fe and Mo), Phys. Chem. Chem. Phys. 19 (2017) 30128–30138, doi:10.1039/C7CP05533A.

[36] R. Gostynski, M.M. Conradie, R.Y. Liu, J. Conradie, Electronic influence of different β-diketonato ligands on the electrochemical Behavior of tris (β-diketonato) M (III) complexes, M= Cr, Mn, and Fe, J. Nano Res. 44 (2016) 252–264, doi:10.4028/www.scientific.net/JNanoR.44.252.

[37] M. Wörle, C.P. Guntlin, L. Gyr, M.T. Sougrati, C.H. Lambert, K.V. Kravchyk, R. Zenobi, M.V. Kovalenko, Structural evolution of iron (III) trifluoroacetate upon thermal decomposition: chains, layers, and rings, Chem. Mater. 32 (2020) 2482–2488, doi:10.1021/acs.chemmater.9b05004.

[38] A. Kurutos, O. Ryzhova, U. Tarabara, V. Trusova, G. Gorbenko, N. Gadjev, T. Deligeorgiev, Novel synthetic approach to near-infrared heptamethine cyanine dyes and spectroscopic characterization in presence of biological molecules, J. Photochem. Photobiol. A Chem. 328 (2016) 87–96, doi:10.1016/j.jphotochem.2016.05.019.

[39] N.C. Pernicone, J.B. Geri, J.T. York, Using a combination of experimental and computational methods to explore the impact of metal identity and ligand field strength on the electronic structure of metal ions, J. Chem. Educ. 88 (2011) 1323–1327, doi:10.1021/ed1010079.

[40] I. Diaz-Acosta, J. Baker, J.F. Hinton, P. Pulay, Calculated and experimental geometries and infrared spectra of metal tris-acetylacetonates: vibrational spectroscopy as a probe of molecular structure for ionic complexes. Part II, Spectrochim. Acta A 59 (2003) 363–377, doi:10.1016/S1386-1425(02)00166-X.

[41] I. Diaz-Acosta, J Baker, W. Cordes, P. Pulay, Calculated and experimental geometries and infrared spectra of metal tris-acetylacetonates: vibrational spectroscopy as a probe of molecular structure for ionic complexes. Part I, J. Phys. Chem A 105 (2001) 238–244, doi:10.1021/jp0028599.

[42] U.A. Jayasooriya, J.N. Peck, J.E. Barclay, S.M. Hardy, A.I. Chumakov, D.J. Evans, C.J. Pickett, V.S. Oganesyan, Nuclear inelastic scattering spectroscopy of tris (acetylacetonate) iron (III); a vibrational probe via the iron atom, Chem. Phys. Lett. 518 (2011) 119–123, doi:10.1016/j.cplett.2011.10.063.

[43] M. Kabak, A. Elmali, S. Ozbey, O. Atakol, A. Kenar, Redetermination of the crystal structure of tris(acetylacetonato)iron(III)(ferric acetylacetonate), $C_{30}H_{42}Fe_2O_{12}$, Z. Kristallogr. 211 (1996) 831–832, doi:10.1524/zkri.1996.211.11.831.

[44] P.A. Stabnikov, N.V. Pervukhina, I.A. Baidina, L.A. Sheludyakova, S.V. Borisov, On the symmetry of iron (III) tris-acetylacetonate crystals, J. Struct. Chem. 48 (2007) 186–192, doi:10.1007/s10947-007-0030-z.

[45] M.J. Frisch, G.W. Trucks, H.B. Schlegel, G.E. Scuseria, M.A. Robb, J.R. Cheeseman, G. Scalmani, V. Barone, B. Mennucci, G.A. Petersson, H. Nakatsuji, M. Caricato, X. Li, H.P. Hratchian, A.F. Izmaylov, J. Bloino, G. Zheng, J.L. Sonnenberg, M. Hada, M. Ehara, K. Toyota, R. Fukuda, J. Hasegawa, M. Ishida, T. Nakajima, Y. Honda, O. Kitao, H. Nakai, T. Vreven, J.A. Montgomery, J.E. Peralta, F. Ogliaro, M. Bearpark, J.J. Heyd, E. Brothers, K.N. Kudin, V.N. Staroverov, R. Kobayashi, J. Normand, K. Raghavachari, A. Rendell, J.C. Burant, S.S. Iyengar, J. Tomasi, M. Cossi, N. Rega, J.M. Millam, M. Klene, J.E. Knox, J.B. Cross, V. Bakken, C. Adamo, J. Jaramillo, R. Gomperts, R.E. Stratmann, O. Yazyev, A.J. Austin, R. Cammi, C. Pomelli, J.W. Ochterski, R.L. Martin, K. Morokuma, V.G. Zakrzewski, G.A. Voth, P. Salvador, J.J. Dannenberg, S. Dapprich, A.D. Daniels, O. Farkas, J.B. Foresman, J.V. Ortiz, J. Cioslowski, D.J. Fox, Gaussian 09, Revision A.02, Gaussian Inc., Wallingford CT, 2009.

[46] A.D. Becke, Density-functional thermochemistry. III. The role of exact exchange, J. Chem. Phys. 98 (1993) 5648–5652.

[47] C. Lee, W. Yang, R.G. Parr, Development of the colle-salvetti correlation-energy formula into a functional of the electron density, Phys. Rev. B 37 (1988) 785–789, doi:10.1103/PhysRevB.37.785.

[48] V. Enchev, N. Gadjev, I. Angelov, S. Minkovska, A. Kurutos, N. Markova, T. Deligeorgiev, Green synthesis, structure and fluorescence spectra of new azacyanine dyes, J. Mol. Struct. 1147 (2017) 380–387, doi:10.1016/j.molstruc.2017.06.119.

[49] R.D. Dennington, T.A. Keith, J.M. Millam, GaussView 6.0. 16, Semichem. Inc., Shawnee Mission KS, 2016.

[50] F.W. BieglerKonig, J. Schonbohm, D. Bayles, Software news and updates AIM2000, J. Comput. Chem. 22 (2001) 545–559.

[51] M.H. Jamróz, Vibrational Energy Distribution Analysis: VEDA 4 Program, Warsaw, Poland, 2004.

[52] M.H. Jamróz, Vibrational energy distribution analysis (VEDA): scopes and limitations, Spectrochim. Acta A 114 (2004) 220–230.

[53] V. Darugar, M. Vakili, S.F. Tayyari, F.S. Kamounah, Validation of potential energy distribution by VEDA in vibrational assignment some of β-diketones; comparison of theoretical predictions and experimental vibration shifts upon deutration, J. Mol. Gr. Model. 107 (2021) 107976, doi:10.1016/j.jmgm.2021.107976.

[54] R.C. Fay, T.S. Piper, Coördination compounds of trivalent metals with unsymmetrical bidentate ligands. II. Trifluoroacetylacetonates, J. Am. Chem. Soc. 85 (1963) 500–504, doi:10.1021/ja00888a002.

[55] M.K. Chaudhuri, S.K. Ghosh, Novel synthesis of tris (acetylacetonato) iron (III), J. Chem. Soc. Dalton Trans. (1983) 839–840, doi:10.1039/DT9830000839.

[56] E.W. Berg, J.T. Truemper, Vapor pressure-temperature data for various metal β-diketone chelates, Anal. Chim. Acta 32 (1965) 245–252, doi:10.1016/S0003-2670(00)88930-8.

[57] B.D. Fahlman, A.R. Barron, Substituent effects on the volatility of metal β-diketonates, Adv. Mater. Opt. Electron. 10 (2000) 223–232, doi:10.1002/1099-0712(200005/10)10:3/5⟨223::AID-AMO411⟩3.0.CO;2-M.

[58] A.A. Petrova, N.V. Tverdova, N.I. Giricheva, G.V. Girichev, Molecular structure of tris (Acetylacetonate) Iron studied by gas-phase electron diffraction and DFT calculations, Izv. Vyssh. Uchebn. Zaved., Khim. Khim. Tekhnol. 60 (2017) 97–99, doi:10.6060/tcct.2017603.5601.

[59] M. Zahedi-Tabrizi, F. Tayyari, Z. Moosavi-Tekyeh, A. Jalali, S.F. Tayyari, Structure and vibrational assignment of the enol form of 1, 1, 1-trifluoro-2, 4-pentanedione, Spectrochim. Acta A 65 (2006) 387–396, doi:10.1016/j.saa.2005.11.019.

[60] S.F. Tayyari, M. Vakili, A.R. Nekoei, H. Rahemi, Y.A. Wang, Vibrational assignment and structure of trifluorobenzoylacetone: a density functional theoretical study, Spectrochim. Acta A 66 (2007) 626–636, doi:10.1016/j.saa.2006.04.002.

[61] D. Dimić, D. Milenković, J. Ilić, B. Šmit, A. Amić, Z. Marković, J.Dimitrić Marković, Experimental and theoretical elucidation of structural and antioxidant properties of vanillylmandelic acid and its carboxylate anion, Spectrochim. Acta A 198 (2018) 61–70, doi:10.1016/j.saa.2018.02.063.
[62] D. Dimić, The importance of specific solvent-solute interactions for studying UV-vis spectra of light-responsive molecular switches, C. R. Chim. 21 (2018) 1001–1010, doi:10.1016/j.crci.2018.09.007.
[63] S. Seshadri, MP. Rasheed, R. Sangeetha, Vibrational spectroscopic (FT-IR and FT-Raman) studies, HOMO LUMO analysis and electrostatic potential surface Of 2-amino-4, 5-dimethyl-3-furancarbonitrile, IOSR J. Appl. Chem. 15 (2015) 87–100, doi:10.9790/5736-088287100.
[64] A.M. Mansour, Coordination behavior of sulfamethazine drug towards Ru (III) and Pt (II) ions: synthesis, spectral, DFT, magnetic, electrochemical and biological activity studies, Inorg. Chim. Acta 394 (2013) 436–445, doi:10.1016/j.ica.2012.08.025.
[65] I. Fleming, Frontier Orbitals and Organic Chemical Reactions, 1st ed., Wiley, New York, 1976.
[66] K. Nakamoto, P.J. McCarthy, A. Ruby, A.E. Martell, Infrared spectra of metal chelate compounds. II. Infrared spectra of acetylacetonates of trivalent metals, J. Am. Chem. Soc. 83 (1961) 1066–1069, doi:10.1021/ja01466a014.
[67] K. Nakamoto, C. Udovich, J. Takemoto, Metal isotope effect on metal-ligand vibrations. IV. Metal complexes of acetylacetone, J. Am. Chem. Soc. 92 (1970) 3973–3976, doi:10.1021/ja00716a024.